

# Application of breakthrough curves to investigate the chemisorption of carbon monoxide and hydrogen gases on platinum/silica catalysts

Mohamed Mokhtar Mohamed \*, Mohamed Ashraf El-Erian

*Al-Azhar University, Faculty of Science, Chemistry Department, Naser City, Cairo, Egypt*

Received 8 December 1994; revised 31 August 1995

## Abstract

A study has been made on the consecutive adsorption of CO/H<sub>2</sub> gases on Pt/SiO<sub>2</sub> catalysts at 523 K using breakthrough measurements. The criteria for dispersion, diffusion and change in the pore size is evaluated and discussed as well as the equilibrium kinetic curves, which show to what extent the rates of sorption of one of the gases is affected by the presence of the other. The changes in average pore radii, surface areas and pore volume were very well estimated and correlated well with the breakthrough data.

*Keywords:* Adsorption; Platinum/silica catalysts; Breakthrough measurements; Carbon monoxide/hydrogen

## 1. Introduction

Measurements of the breakthrough curves of gases adsorbed, in a consecutive way, on supported metal catalysts can provide information about the strength of interaction of these gases with the catalysts as well as equilibrium kinetic curves at high temperatures, which are difficult to obtain by conventional techniques. This information contributes to the understanding of the catalytic processes and how the rates of sorption of the individual components are affected by the presence of the other species.

In spite of the difficulties that can arise for H<sub>2</sub> and CO chemisorption, such as the non-stoichiometry and the existence of several modes, they are still considered the best material for many measurements [1,2].

It is well known that platinum supported on silica shows different behaviour between the two reducing agents, CO and H<sub>2</sub> [3,4]. Therefore, the relative changes in diffusability of CO and H<sub>2</sub> can be evaluated. Since no work has yet been reported on the consecutive adsorption of CO and H<sub>2</sub> gases on Pt/SiO<sub>2</sub> catalysts, a study on the diffusion effect, dispersion, pore size alterations and sorbate-sorbent interactions has been made using breakthrough measurements.

## 2. Experimental

This work was carried out using silica gel 60 (Merck) with a BET surface area 450 m<sup>2</sup> g<sup>-1</sup> loaded with 2 wt.% Pt by an

impregnation technique. The sample was prepared by the dropwise addition to the support material of sufficient aqueous H<sub>2</sub>PtCl<sub>6</sub> (Alfa) of the appropriate concentration to give incipient wetness while being stirred thoroughly with a glass rod. The solid was separated by vacuum filtration through a fritted funnel. The solid was first dried in a vacuum desiccator at room temperature, and then dried at 393 K before calcination at 773 K in air for 10 h.

H<sub>2</sub> and CO (99% purity) adsorption isotherms were measured with a gas volumetric apparatus [5]. The sample was outgassed at 523 K to a residual pressure of 10<sup>-4</sup> torr.

The breakthrough curves were obtained by displacement chromatography. This requires firstly that the adsorbent is very close to the saturation conditions with one of the two gases and secondly that the other gas will be allowed to replace the preadsorbed one at a certain pressure and temperature.

In order to ensure uniform gas distribution, a column (50 cm × 10 mm) was packed with the sample particles and thermostated at 523 K. The volume flow and concentration were kept constant. More details about the chromatograph can be found elsewhere [6].

Particle size distribution was determined by electron microscope on a Jeol 100B instrument. The sample was examined by ultrasonic dispersion in methanol followed by deposition on the grids. The final magnification of 2 000 000 was known to within 5%. The sample diameter was characterized by the mean arithmetic diameter of 1000 particles measured with a Zeiss TGZ3 semi-automatic size analyser.

\* Corresponding author.

Table 1  
Surface characteristics of the calcined silica and Pt loaded silica

Sample	$A_{\text{BET}}$ ( $\text{m}^2 \text{g}^{-1}$ )	$V_{\text{P}}$ ( $\text{ml g}^{-1}$ )	BET-C (constant)	$r_{\text{H}}$ ( $\text{\AA}$ )	$A_{\text{cum}}^{\text{a}}$ ( $\text{m}^2 \text{g}^{-1}$ )		$V_{\text{cum}}$ ( $\text{ml g}^{-1}$ )	
					pp <sup>b</sup>	cp <sup>c</sup>	pp	cp
Silica	450	0.8215	77	18	435	568	0.9	0.8397
Pt/SiO <sub>2</sub>	397	0.7550	80	19	382	430	0.75	0.7840

<sup>a</sup> cum = cumulative.

<sup>b</sup> pp = parallel plate.

<sup>c</sup> cp = cylindrical pore.

Adsorption measurements with liquid nitrogen ( $-195.8^\circ\text{C}$ ) were carried out using a gas volumetric apparatus. The specific surface area  $A_{\text{BET}}$ , total pore volume  $V_{\text{P}}$  (calculated as liquid volume at  $P/P^0 = 0.95$ ), BET-C constant and the average pore radius  $r_{\text{H}} = V_{\text{P}}/A_{\text{BET}}$  for the substrate [7] and Pt/SiO<sub>2</sub> catalyst are given in Table 1.

### 3. Results and discussion

In Fig. 1, the adsorption isotherm of H<sub>2</sub> on Pt/SiO<sub>2</sub> (Type I) catalyst at 523 K, which is relatively consistent with the features of microporous silica studied by others [8], is compared with the breakthrough curve of the same system (Fig. 2). This figure also shows the dependence of the breakthrough shape on the amount of H<sub>2</sub> adsorbed on the Pt/SiO<sub>2</sub> system as evidenced by the broad concave feature i.e. surface diffusivity is suggested. In order to ascertain this, experiments

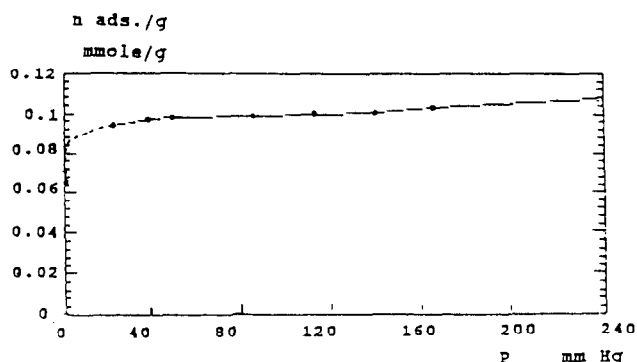


Fig. 1. Adsorption isotherm of H<sub>2</sub> on 2 wt.% Pt/SiO<sub>2</sub> catalyst at 523 K.

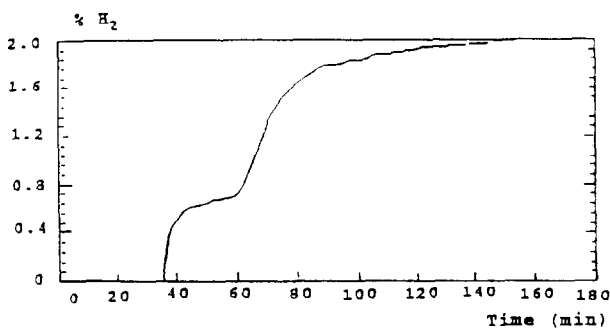


Fig. 2. Breakthrough curve of H<sub>2</sub> on 2 wt.% Pt/SiO<sub>2</sub> catalyst.

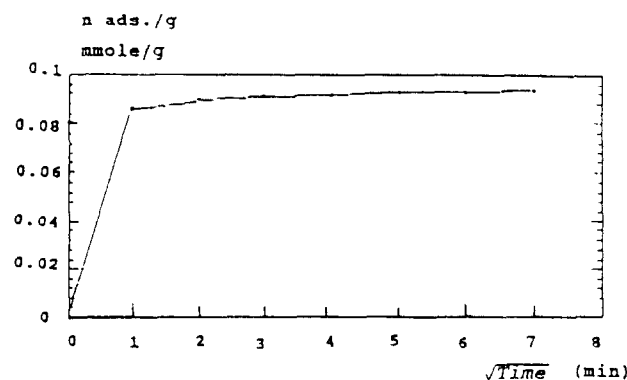


Fig. 3. Kinetic curve of H<sub>2</sub> on 2 wt.% Pt/SiO<sub>2</sub> catalyst.

at different temperatures have been carried out. The diffusion was found to be temperature dependent and indeed the behaviour depicted in Fig. 2 establishes the diffusion phenomena. Consequently, one cannot attribute the breakthrough curve in Fig. 2 to the change in the sticking probability of H<sub>2</sub> as its surface coverage increases. The increase in uptake of H<sub>2</sub> with time (Fig. 2) was marked for the consecutive zones when compared with the uptake resulting from the kinetic curve (Fig. 3).

Thus, we can conclude that the Pt impregnated on silica is heterogeneously distributed and of different pore sizes, and therefore these adsorption sites can react differently with H<sub>2</sub> depending on the difference in binding energies. Electron microscopy has emphasized the same result. A large distribution of particle sizes up to 70  $\text{\AA}$  was seen, although greater than 52% are still less than 8  $\text{\AA}$ . This distribution can be regarded as a guide to the high dispersion reflected from this catalyst. This broad distribution of particle sizes shows a fairly good agreement with the corresponding particle sizes reported by Jackson et al. [9] observed in the high resolution transmission microscopy (HRTEM).

It can be seen also that the saturation coverage shown in Fig. 3 (at about 0.09  $\text{mmol g}^{-1}$ ) has been obtained in 1 min, whereas the total breakthrough, shown in Fig. 2, takes more than 30 min. This can be explained as follows: the bare surface on Pt/SiO<sub>2</sub> catalyst, in Fig. 3, needs a very short time to obtain equilibrium but in Fig. 2 (breakthrough) a surface covered with H<sub>2</sub> already exists, and needs more time for equilibration. By way of comparison, the N<sub>2</sub> adsorption on the parent and Pt/SiO<sub>2</sub> catalyst are illustrated in Fig. 4.

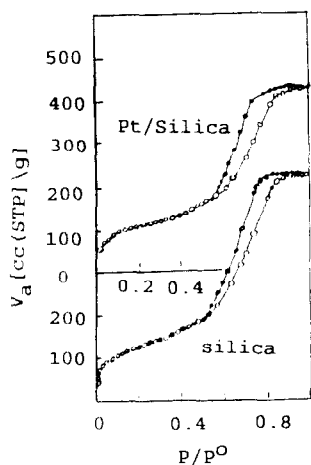


Fig. 4.  $N_2$  adsorption-desorption isotherms (77 K) of parent and Pt loaded silica samples.

Both the parent and Pt/SiO<sub>2</sub> samples resulted in a Type IV isotherm, i.e. a mesoporous solid, whose upward deviation starts at  $P/P^0 = 0.38$  and  $0.44$ , respectively. The hysteresis loop shows a type H1 character at the higher regions for both samples, where the two branches are parallel to each other, and which can be attributed to a cylindrical pore shape [10]. Fig. 4 also presents a region for capillary condensation, which is formulated from the upward deviation (evaluated from the  $v-t$  plot). This plot also depicts a region for reversible capillary condensation in the range of  $P/P^0 = 0.51$  (where the hysteresis loop closes) and  $P/P^0 = 0.38$  (where the upward deviation commences). This reversible capillary condensation can take place in pores of cone and wedge shape having [10] the sizes of wide micropores and/or narrow mesopores [11].

Table 1 shows the cumulative parameters of volume and area in which an agreement between experimental and calculated values is favoured for the parallel plate model. Furthermore, the apparent decrease in area is found to be more important than the decrease in pore volume where the average pore radius shows an increase upon Pt addition (Table 1). This can be explained as follows: at such a low loading the Pt particles can reside in the narrow pores of silica, characterized by a high surface-to-volume ratio, in which the interaction with surface hydroxyl groups and the detachment of weakly bound species takes place.

In comparison with adsorption isotherm of H<sub>2</sub> on Pt/SiO<sub>2</sub> (Fig. 1), it can be deduced through the appearance of a Type IV ( $N_2$  non-specific adsorption) and a Type I (H<sub>2</sub> specific adsorption), that a Pt/SiO<sub>2</sub> catalyst is accessible for both microporosity as well as mesoporosity.

The obvious similarity shown in Fig. 4, in the isotherm shape and behaviour provides a means of calculating the average pore radii through the difference in  $r_H$  values ( $= V_p/A_{BET}$ ) formulated from the  $N_2$  and H<sub>2</sub> isotherms. Therefore, the average pore radius is in the range of  $19 \leq r_H < 10$ . The breakthrough curve of CO on the Pt/SiO<sub>2</sub> catalyst shows only one fast jump (Fig. 5). This indicates

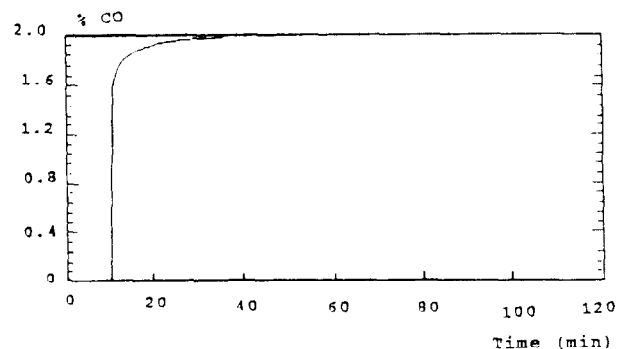


Fig. 5. Breakthrough of CO on 2 wt.% Pt/SiO<sub>2</sub> catalyst.

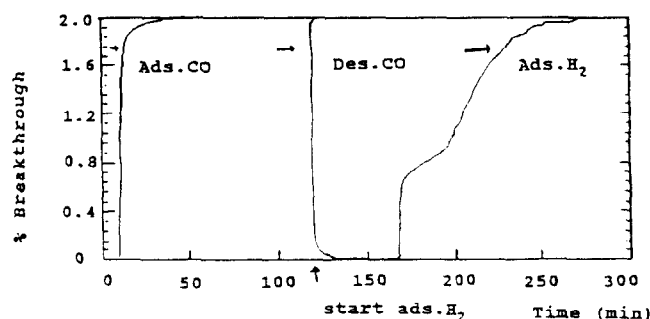


Fig. 6. Breakthrough curve of CO preadsorbed on 2 wt.% Pt/SiO<sub>2</sub> followed by H<sub>2</sub> adsorption.

that only one site can be available when CO is adsorbed on the Pt/SiO<sub>2</sub> catalyst i.e. a diffusion-controlled process as a result of the homogeneity of the Pt particles on the silica surface when exposed to CO adsorption.

This latter conclusion is consistent with the infrared (IR) results showing that CO adsorbed on a Pt surface at high temperatures (523 K) exhibits only a linear band [12,13] whereas H<sub>2</sub> adsorbed on Pt exhibits two types of adsorption bands [14]. As can be seen, the surface diffusivity of H<sub>2</sub> is higher than that of CO probably because H<sub>2</sub> blockage is more severe due to the high kinetic energy at such high temperature compared with CO molecules. The molecular area of H<sub>2</sub> is smaller than that of CO which might be another plausible explanation for this behaviour. Similarly, the heterogeneity of the adsorbent, as a result of H<sub>2</sub> adsorption, might constitute another reason [9].

In Fig. 6, the breakthrough curve of the adsorption of H<sub>2</sub> on Pt/SiO<sub>2</sub> saturated with CO at 523 K is compared with the single breakthrough curves in Figs. 2 and 5. The H<sub>2</sub> molecules displace the already adsorbed CO molecules until mixture equilibrium is reached. When H<sub>2</sub> breakthrough occurs, the CO concentration decreases to the initial concentration. A constant pattern of behaviour for H<sub>2</sub> is observed in Fig. 6, with a significant increase in the first zone uptake compared with the single breakthrough analogue (Fig. 2).

This could be attributed to the enhancement of this site, responsible for creating the first zone, as a result of the interaction of Pt with CO at the beginning, however, the accessibility of this site for more H<sub>2</sub> adsorption does occur. Fig. 6 also shows that the total amount of CO adsorbed by H<sub>2</sub> equal

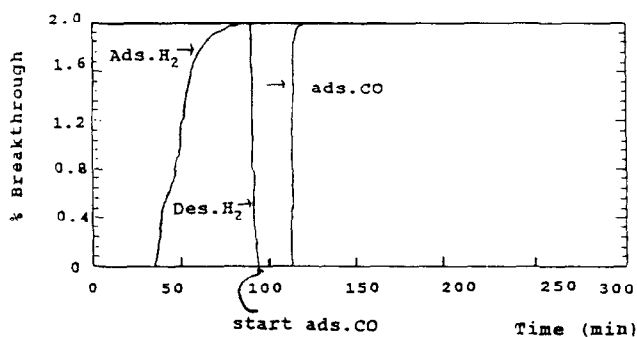


Fig. 7. Breakthrough curve of  $H_2$  preadsorbed on 2 wt.% Pt/SiO<sub>2</sub> followed by CO adsorption.

to the amount of CO that was initially desorbed. This means that the probability of finding CO molecules still sticking on the surface when  $H_2$  breakthrough occurs is negligible. This is also supported by the similar pattern of behaviour of  $H_2$  after CO desorption has been completed.

Fig. 7 shows the breakthrough curve of CO adsorbed on Pt/SiO<sub>2</sub> saturated with  $H_2$ . Corresponding to the adsorption capacity from the single breakthrough (Fig. 1),  $H_2$  breaks through first during adsorption. The following CO mass transfer zone displaces the already adsorbed  $H_2$  molecules and an increase in  $H_2$  outlet concentration takes place. The earlier desorption of  $H_2$  (Fig. 7) compared with that of CO (Fig. 6) implies that the adsorption capacities are not in the same order of magnitude. This could emphasize that the weakly adsorbed component  $H_2$  is being displaced in a relatively shorter equilibrium time, compared with CO which showed nearly identical adsorption and desorption profiles. It is of interest to note that the constant pattern of behaviour of  $H_2$  changes when CO adsorption takes place.

Another reason for the earlier desorption of  $H_2$  could be that the more weakly adsorbed  $H_2$  has a higher mobility in the adsorbed phase than the strongly adsorbed CO. From this, we have concluded that the adsorption sites available for CO molecules on Pt/SiO<sub>2</sub> are very limited (one site) but stronger CO adsorption during breakthrough is confirmed. Contrarily, two adsorption sites are developed as a result of an incomplete reduction by  $H_2$ .

The greater interaction of the CO molecules compared with the  $H_2$  molecules with the Pt/SiO<sub>2</sub> surface reflects the greater dispersion of Pt ions reduced by CO molecules than that of  $H_2$  molecules. It seems that the changes in Pt dispersion upon CO adsorption creates a diffusion-controlled system.

It is also evident that the adsorption of CO prior to  $H_2$  could help in enhancing the adsorbability of one of the two sites, (Fig. 6, first zone). This is confirmed by  $H_2$  breakthrough on increasing the accessibility of this site during  $H_2$  adsorption. It is also possible that a substantial amount of  $H_2$  can be produced as a result of the interaction of CO (ads) with the

OH of the support, at such a high temperature in order to enhance the adsorption ability of the first zone. This result was consistent with the findings of Jackson et al. [15].

It is obvious, in Fig. 7, that the concentration of  $H_2$  on the surface when CO breakthrough occurs is almost zero because CO molecules start to occupy the preadsorbed sites with high bonding forces and, as a result, a fade feature (two zones) for the  $H_2$  molecules is obtained owing to their weaker adsorption and higher mobility. Further information can also be deduced. The incomplete profile of  $H_2$  desorption in Fig. 7 and the earlier adsorption of CO could prove that CO occupies sites that were available to  $H_2$ . This can only be obtained when  $H_2$  is preadsorbed on the catalyst followed by CO adsorption. In contrast, when CO is preadsorbed,  $H_2$  takes a comparatively long time before it reaches the prominent profile shown in Fig. 6. From this, it seems that the primary interaction of CO with the catalyst could result in a surface restructuring or a reduction in the activation energy barrier for the next incoming gas and an enhancement in the  $H_2$  adsorption profile should be seen.

Although the molecular area of CO is relatively higher than that of  $H_2$ , the CO molecules that are eventually displaced by  $H_2$  are more strongly adsorbed than the  $H_2$  molecules. This could be attributed to the increasing dipolar interactions of the linearly adsorbed CO with the Pt/SiO<sub>2</sub> system [16].

## References

- [1] X. Xiaoding, E.B.M. Doesburg and J.J.F. Scholten, *Catal. Today*, 2 (1987) 125.
- [2] M.M. Mohamed, *J. Mater. Science*, (1995) in press.
- [3] R. Barth and A. Ramachandran, *J. Catal.*, 125 (1990) 467.
- [4] J.E. Benson, H.S.H. Wang and M. Boudart, *J. Catal.*, 30 (1973) 146.
- [5] M.M. Mohamed, *Spectrochimica Acta A*, 51 (1995) 1.
- [6] M. Suzuki and J.M. Smith, in J.C. Griddings (ed.), *Advances in Chromatography*, Marcel Dekker, New York, 13th edn., 1975, pp. 214–262.
- [7] G.M.S. El Shafei and M.M. Mohamed, *Colloids Surf.*, 94 (1995) 267.
- [8] S.J. Gregg and K.S.W. Sing, *Adsorption, Surface Area and Porosity*, 2nd edn., Academic Press, New York, 1982, pp. 195–198.
- [9] S.D. Jackson, J. Willis, G.D. McLellan, G. Webb, M.B.T. Keegan, R.B. Moyes, S. Simpson, P.B. Wells and R. Whyman, *J. Catal.*, 139 (1993) 191.
- [10] J.H. Boer and B.C. Lippens, *J. Catal.*, 3 (1964) 38.
- [11] S.J. Gregg and K.S.W. Sing, *Adsorption, Surface Area and Porosity*, 2nd edn., Academic Press, New York, 1982, pp. 129–163.
- [12] J. Sarknary and R.D. Gonzalez, *Appl. Catal.*, 4 (1982) 53.
- [13] P.B. Wells, *Appl. Catal.*, 18 (1985) 259.
- [14] K. Tamaru, *Dynamic Heterogeneous Catalysis*, Academic Press, New York, 1978, p. 54.
- [15] S.D. Jackson, B.M. Glanville, J. Willis, G.D. McLellan, G. Webb, R.B. Moyes, S. Simpson, P.B. Wells and R. Whyman, *J. Catal.*, 139 (1993) 207.
- [16] B. Lang, R.W. Joyner and G.A. Somorjai, *Surf. Sci.*, 30 (1972) 454.